Sergey N. Krylov

Department of Chemistry,
York University,
Toronto, Ontario, Canada

Received September 11, 2006
Revised October 21, 2006
Accepted October 21, 2006

Review

Kinetic CE: Foundation for homogeneous kinetic affinity methods

Kinetic capillary electrophoresis (KCE) is defined as capillary electrophoresis of species that interact during electrophoresis. KCE can serve as a conceptual platform for development of homogeneous kinetic affinity methods for affinity measurements (measurements of binding parameters and quantitative measurements) and affinity purification (purification of known molecules and search of unknown molecules). A number of different KCE methods can be designed by varying initial and boundary conditions – the way interacting species enter and exit the capillary. KCE methods will find multiple practical applications in the designing of biomedical diagnostics and the development of drug candidates. Here, the concept of KCE, its up-to-date applications, and future prospective are reviewed.

Keywords: Affinity measurements / Affinity purification / Kinetic CE
DOI 10.1002/elps.200600577

1 Introduction

1.1 Affinity interactions

Affinity interaction is highly selective non-covalent binding of molecules at least one of which is a biopolymer. Affinity interactions play a very important role in biology: they control cell recognition, signal transduction, immune response, DNA replication, gene expression, *etc*. Affinity interactions are also pivotal to a number of widely used technologies including immunoassays, hybridization analyses, affinity purification, sensors, fluorescent staining, selection of drug candidates and affinity probes from combinatorial libraries, *etc*. In this review, two molecules capable of affinity interactions will be called a target (T) and a ligand (L). When diagnostic or therapeutic applications are discussed, by default, T will be assigned to diagnostic and therapeutic targets and L will be assigned to their affinity partners (*e.g.*, diagnostic probes and affinity ligands). Affinity interaction of L and T with the formation of an affinity complex (L·T or C) is described by the following equation:

$$\mathrm{L} + \mathrm{T} \underset{k_{\mathrm{off}}}{\overset{k_{\mathrm{on}}}{\rightleftharpoons}} \mathrm{L{\cdot}T}$$

or

$$\mathrm{L} + \mathrm{T} \underset{k_{\mathrm{off}}}{\overset{k_{\mathrm{on}}}{\rightleftharpoons}} \mathrm{C} \qquad (1)$$

where k_{on} and k_{off} are rate constants of complex formation and dissociation, respectively. In this review, L·T and C are used interchangeably to denote the complex; L·T is used to emphasize the non-covalent nature of the complex and C is used to simplify mathematical expressions. Complex stability is typically described in terms of the equilibrium dissociation constant, $K_d = k_{off}/k_{on}$ (or in terms of the equilibrium binding constant, $K_b = 1/K_d$). Studies of affinity interactions or the use of affinity interactions for other purposes are performed with affinity methods.

1.2 Affinity methods

Affinity methods play an important role in biomolecular sciences. Their applications include affinity measurements (studies of biomolecular interactions and quantita-

Correspondence: Professor Sergey N. Krylov, Department of Chemistry, York University, Toronto, Ontario, Canada M3J 1P3
E-mail: skrylov@yorku.ca
Fax: +1-416-736-2100

Abbreviations: cNECEEM, continuous NECEEM; **ECEEM**, equilibrium CE of equilibrium mixtures; **KCE**, kinetic CE; **L**, ligand; **L·T** or **C**, non-covalent ligand-target complex; **NECEEM**, non-equilibrium CE of equilibrium mixtures; **ppKCE**, plug-plug KCE; **SELEX**, systematic evolution of ligands by exponential enrichments; **SPR**, surface plasmon resonance; **SSB**, ssDNA-binding protein; **sSweepCE**, short SweepCE; **sSweepCEEM**, short SweepCE of equilibrium mixtures; **SweepCE**, sweeping CE; **T**, target

tive analyses of biomolecules) and affinity purification (purification of known molecules and search of unknown molecules) [1–4]. The major industrial uses of affinity methods are in biomedical diagnostics and drug development [5, 6].

Affinity methods can be classified in a number of ways. One of the classifications distinguishes separation-free and separation-based affinity methods. Separation-free methods are suitable only for affinity measurements, while separation-based methods can facilitate both affinity measurements and affinity purification. Here we only consider separation-based affinity methods.

1.2.1 Heterogeneous *vs.* homogeneous methods

In separation-based methods, L (or T) is physically separated from L·T. Separation-based methods can be further classified as heterogeneous or homogeneous, depending on how separation of L from L·T is achieved (Fig. 1). In heterogeneous methods, L is separated from L·T on the surface of a solid substrate, such as a filter, chromatographic support, or a sensor [7–9]. In homogeneous methods, L is separated from L·T in solution based on differences in the mobility of L and L·T. A differential mobility in solution can be induced by centrifugal or electrostatic forces [10–12]. Both heterogeneous and homogeneous approaches have advantages and limitations. The common drawback for all heterogeneous methods is nonspecific binding of L to the surface. Methods that require immobilization of T (or L) on the surface are characterized by additional limitations. Depending on the type of immobilized molecules, the immobilization procedure

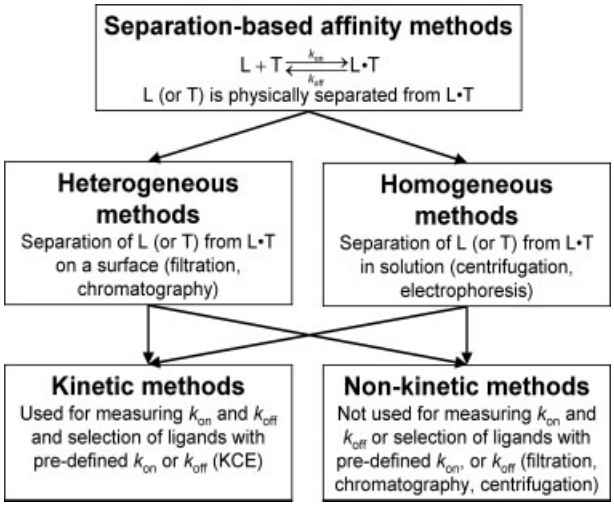

Figure 1. Classification of separation-based affinity methods.

can be challenging, expensive, and time consuming. Molecules immobilized on the surface often degrade rapidly, thus decreasing the reliability of the method with increasing the cost of analyses. In addition, immobilization can change the affinity of L to T, making the results of measurements inaccurate [13]. Finally, due to the complexity of reactions on the surface, heterogeneous methods are difficult to model in detail mathematically. The advantage of heterogeneous methods is the simplicity of separation; since T is fixed on the surface, separation of L from L·T is trivial. Therefore, heterogeneous methods are great for routing affinity purification. The major limitation of homogeneous methods is the need for finding suitable conditions to separate L from L·T in solution. However, for affinity measurements and advanced affinity purification homogeneous methods are preferable over heterogeneous.

1.2.2 Kinetic *vs.* non-kinetic methods

Separation-based affinity methods can also be categorized as kinetic or non-kinetic (see Fig. 1). Kinetic methods are those that do not assume equilibrium in reaction (1) and can, thus, be used for measuring k_{on} and k_{off} and selection of binding ligands with pre-determined k_{on} and k_{off}. In addition, kinetic methods can be used for quantitative affinity analyses of targets (measuring concentrations of T) with "weak" affinity probes (high k_{off}). Non-kinetic methods, in contrast, assume equilibrium and, thus, are not used for these tasks. It should be emphasized, that the assumption of equilibrium in non-kinetic methods is somewhat artificial and not theoretically required. Furthermore, strictly speaking equilibrium cannot be maintained in separation-based affinity methods as separation disturbs equilibrium. All non-kinetic methods can be potentially converted into kinetic methods by modifying experimental settings and approaches to data analysis.

Among conventional separation-based affinity methods only surface plasmon resonance (SPR) could be characterized as a kinetic method [14]. It facilitates direct measurements of K_d and k_{off} values; the k_{on} value can be then calculated, $k_{on} = k_{off}/K_d$. SPR is currently the major platform for studying kinetics of non-covalent biomolecular interactions [15, 16]. It can be potentially used for selection of binding ligands with pre-defined binding parameters from combinatorial libraries. However, SPR is a heterogeneous method with all the limitations and drawbacks associated with heterogeneous methods in general. Our recent work has focused on the development of kinetic capillary electrophoresis (KCE), which serves as a conceptual platform for the first generation of homoge-

neous kinetic separation-based affinity methods [17–40]. This is the first comprehensive review of KCE, which covers the concept of KCE and its multiple fundamental applications.

2 The concept of KCE

2.1 Theoretical bases of KCE

CE is an instrumental platform of KCE. CE is a mature analytical technique with tens of thousands of papers published and hundreds of patents issued over the last two decades. CE can be advantageously interfaced with all types of quantitative detection: optical, electrochemical, and mass spectrometric. The method can be performed either in capillaries or in channels on microchips. Commercially available instrumentation supports virtually all developed modes and formats of CE. Practical applications of CE range from analysis of all classes of molecules to genome sequencing and analyses of single cells. Despite such a great progress in CE in general, its capabilities as a base of kinetic affinity methods had not been realized prior to our introducing KCE methods. Pre-KCE work on kinetic applications of CE to affinity interactions is virtually limited to a single study by Whitesides and co-authors [41].

KCE is defined as CE separation of species, which interact during electrophoresis. It should be noted, that, strictly speaking, KCE is a non-equilibrium concept as it is impossible to maintain equilibrium during separation. KCE involves two major processes: affinity interaction of L and T, described by Eq. (1), and separation of L, T, and C based on differences in their electrophoretic velocities, v_L, v_T, and v_C. These two processes are described by the following general system of partial differential equations:

$$\begin{aligned}
&\frac{\partial L(t,x)}{\partial t} + \upsilon_L \frac{\partial L(t,x)}{\partial x} = -k_{on} L(t,x) T(t,x) + k_{off} C(t,x) \\
&\frac{\partial T(t,x)}{\partial t} + \upsilon_L \frac{\partial T(t,x)}{\partial x} = -k_{on} L(t,x) T(t,x) + k_{off} C(t,x) \qquad (2) \\
&\frac{\partial C(t,x)}{\partial t} + \upsilon_L \frac{\partial C(t,x)}{\partial x} = -k_{off} C(t,x) + k_{on} L(t,x) T(t,x)
\end{aligned}$$

where L, T, and C are concentrations of L, T, and C, respectively; t is the time passed since the beginning of separation; x is the distance from the injection end of the capillary. System 2 describes the two basic processes that are always present in KCE. Depending on the species studied and the specific analytical setup, other processes, such as binding with complex stoichiometry, diffusion, adsorption to capillary walls, *etc.* can play significant roles in KCE. In such cases, mathematical terms, describing additional processes, must be added to system 2. The solution of system 2 depends on the initial and boundary conditions: initial distribution of L, T, and C along the capillary and the way L, T, and C are introduced into the capillary and removed from the capillary during separation. This solution can be found non-numerically for specific sets of initial and boundary conditions and specific assumptions [17, 18, 26]. For KCE to be a generic approach, it is required that system 2 be solved for any set of conditions; such solutions can be found only numerically.

2.2 Designing KCE methods by changing initial and boundary conditions

Every set of qualitatively unique initial and boundary conditions for system 2 defines a unique KCE method. Table 1 compares seven previously published KCE methods. Every method has a unique and descriptive name: non-equilibrium capillary electrophoresis of equilibrium mixtures (NECEEM) [17–32], sweeping capillary electrophoresis (SweepCE) [17, 33], continuous NECEEM (cNECEEM) [17], short SweepCE (sSweepCE) [17], plug-plug KCE (ppKCE) [17, 34], short SweepCE of equilibrium mixtures (sSweepCEEM) [17], and equilibrium capillary electrophoresis of equilibrium mixtures (ECEEM) [30, 35–38]. Dynamic kinetic capillary isoelectric focusing (DKCIEF), the most recent KCE method, is not presented here, as it has not been published yet (Liu, Z., Drabovich, A.P., Krylov, S.N., Pawliszyn, J., *Anal. Chem.* 2007, in press). The first column in the table contains drawings, which schematically illustrate initial and boundary conditions. The second and third columns show the mathematical representation of initial and boundary conditions, respectively. The last column contains representative functions $L(t)$, $T(t)$, and $C(t)$ for a fixed x for each method. The notion of "equilibrium mixture" refers to the mixture of L, T, and C at equilibrium, typically prepared outside the capillary. However, the recent invention of a generic method for mixing solutions inside the capillary, which is called transverse diffusion of laminar flow profiles (TDLFP), allows controlled preparation of the equilibrium mixture inside the capillary [39]. The concentrations of the three components, $\widetilde{T}$, $\widetilde{L}$ and $\widetilde{C}$, in the equilibrium mixture are interconnected through the equilibrium dissociation constant, K_d, as $K_d = (\widetilde{T}\widetilde{L}/\widetilde{C})$. As an example, we assume than $v_T > v_L$. New KCE methods can be designed by arbitrarily selecting new qualitatively different sets of initial and boundary conditions.

In NECEEM, a short plug of the equilibrium mixture is injected into the inlet of the capillary, which is pre-filled with the run buffer. Separation is carried out with both inlet

Table 1. KCE methods

KCE method	Schematic representation of initial and boundary conditions	Initial Conditions[a]	Boundary conditions	Simulated concentration profiles
NECEEM	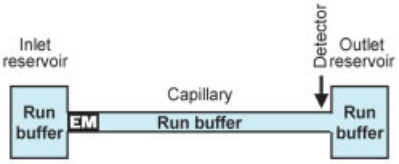	$T(0,x)=\tilde{T}\theta(x)\theta(l-x)$ $L(0,x)=\tilde{L}\theta(x)\theta(l-x)$ $C(0,x)=\tilde{C}\theta(x)\theta(l-x)$ $K_d=\tilde{T}\tilde{L}/\tilde{C}$	$T(t,0)=0$ $L(t,0)=0$ $C(t,0)=0$	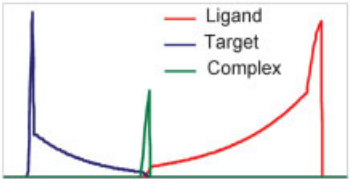
SweepCE		$T(0,x)=\tilde{T}$ $L(0,x)=0$ $C(0,x)=0$	$T(t,0)=\tilde{T}$ $L(t,0)=0$ $C(t,0)=0$	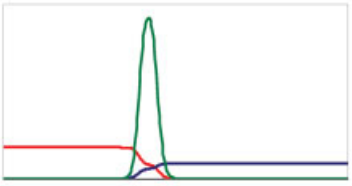
cNECEEM		$T(0,x)=0$ $L(0,x)=0$ $C(0,x)=0$	$T(t,0)=\tilde{T}$ $L(t,0)=\tilde{L}$ $C(t,0)=\tilde{C}$ $K_d=\tilde{T}\tilde{L}/\tilde{C}$	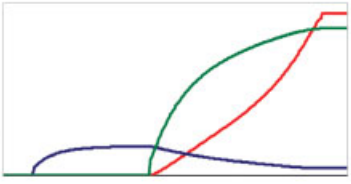
sSweepCE		$T(0,x)=\tilde{T}\theta(x)\theta(l-x)$ $L(0,x)=\tilde{L}\theta(x-l)$ $C(0,x)=0$	$T(t,0)=0$ $L(t,0)=0$ $C(t,0)=0$	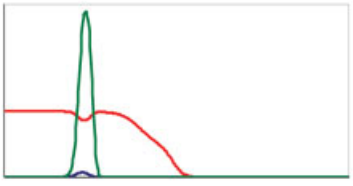
ppKCE		$T(0,x)=\tilde{T}\theta(x)\theta(l_T-x)$ $L(0,x)=\tilde{L}\theta(x-l_L)\times$ $\times\theta(l_T+l_L-x)$ $C(0,x)=0$	$T(t,0)=0$ $L(t,0)=0$ $C(t,0)=0$	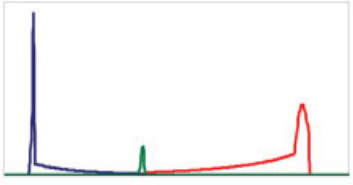
sSweepCEEM		$T(0,x)=\tilde{T}_1\theta(x)\theta(l-x)+$ $+\tilde{T}_2\theta(x-l)$ $L(0,x)=\tilde{L}\theta(x-l)$ $C(0,x)=\tilde{C}\theta(x-l)$ $K_d=\tilde{T}_2\tilde{L}/\tilde{C}$	$T(t,0)=0$ $L(t,0)=0$ $C(t,0)=0$	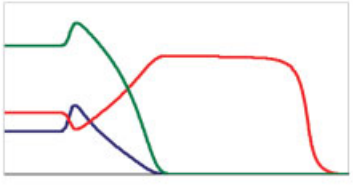
ECEEM		$T(0,x)=\tilde{T}\theta(x)\theta(l-x)$ $L(0,x)=\tilde{L}\theta(x-l)$ $C(0,x)=\tilde{C}\theta(x-l)$ $K_d=\tilde{T}\tilde{L}/\tilde{C}$	$T(t,0)=\tilde{T}$ $L(t,0)=0$ $C(t,0)=0$	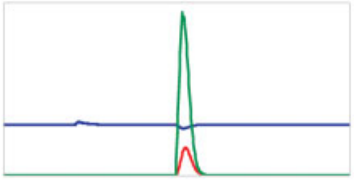
				Migration time to the detector

[a] $\tilde{T}$, $\tilde{L}$, and $\tilde{C}$ are initial concentrations of the target, ligand, and the complex, respectively, in solutions or in the equilibrium mixture (EM), l is the length of the corresponding injected plug, and $\theta(x)$ is a function which equals to 1 when $x > 0$ and equals to 0 when $x \leq 0$.

and outlet reservoirs containing the run buffer only. C continuously dissociates during electrophoresis. If separation is efficient, re-association of T and L can be neglected. The resulting concentration profiles (time dependencies of concentrations for a fixed *x*) contain three peaks of T, C, and L and two exponential "smears" of L and T, which occur from the dissociation of C.

In SweepCE, the capillary is filled with L, while the inlet reservoir contains T and the outlet reservoir contains a run buffer. During electrophoresis, T continuously moves through L, causing continuous binding of T to L. Although binding is a prevalent process in SweepCE, dissociation of C can also contribute to the resulting concentration profiles, which contain a single peak of C and plateaus of T and L.

In cNECEEM, the inlet reservoir is filled with the equilibrium mixture, while the capillary and the outlet reservoir contain the run buffer. During electrophoresis, C is separated from T, which moves faster, and from L, which moves slower. As a result, C continuously dissociates inside the capillary. Although dissociation is a prevalent process in cNECEEM, re-association can also contribute to the resulting concentration profiles, which are represented by smooth functions of $T(t)$, $L(t)$, and $C(t)$ with no pronounced peaks.

In sSweepCE, a short plug of T is injected into the capillary pre-filled with L. Both inlet and outlet reservoirs contain the run buffer. T moves through L during electrophoresis causing both association of T and L and dissociation of resulting C to occur. The concentration profiles of T and C are peak-like, while that of L is a smooth function.

In ppKCE, the plugs of L and T are injected into the capillary pre-filled with the run buffer. The inlet and outlet reservoirs contain the run buffer as well. During electrophoresis, T moves through L, causing the formation of C. When the zone of T passes L, C starts to dissociate. ppKCE can be considered as a functional hybrid of NECEEM and sSweepCE. The resulting concentration profiles resemble those of NECEEM with a smaller peak of C and "smears" of T and L.

In sSweepCEEM, a short plug of T is injected into the capillary pre-filled with the equilibrium mixture. Both inlet and outlet reservoirs contain the run buffer. During electrophoresis, an intricate interplay of dissociation of C and association of T and L occur resulting in sophisticated concentration profiles containing peaks and plateaus.

In ECEEM, a short plug of the equilibrium mixture is injected into the inlet of the capillary, which is pre-filled with solution of T at the same concentration as that in the equilibrium mixture. Separation is carried out with both inlet and outlet reservoirs containing the same solution of T.

2.3 KCE mathematics

2.3.1 General solution: numerical approach

In general, the numerical simulation of electrophoresis is challenging. The difficulties are associated with the incompatibility of a single "space" grid with different velocities of separated species, whose electrophoretic peaks may have sharp fronts. All conventional methods of electrophoretic simulations rely on using a single grid for x, $x = n\,\Delta x$, where Δx is the length of the x increment and n is an integer representing the point number in calculations. The grid is usually associated with the velocity, v, of one of the separated species: $x = \Delta x + v\Delta t$, where Δt is the time increment. As a result, the species, which migrate with velocities different from v, are simulated "out of the grid". This leads to rounding errors that are severely aggravated by sharp fronts of electrophoretic peaks [42, 43]. This problem was addressed by developing a multi-grid algorithm for solving system 2 with an individual Δx for every one of the three components [17]:

$$\begin{aligned} \Delta x_L &= v_L \Delta t \\ \Delta x_T &= v_T \Delta t \\ \Delta x_C &= v_C \Delta t \end{aligned} \qquad (3)$$

The multi-grid algorithm can be used to write a computer program, which calculates $L(t,x)$, $T(t,x)$, and $C(t,x)$. These dependencies can, in turn, be used to build simulated electropherograms, which can be compared with experimental ones. The multi-grid approach provides a new powerful tool for modeling chromatographic and electrophoretic data. It tolerates sharp fronts of peaks typical for chromatograms and electropherograms and increases the speed of calculations.

2.3.2 Simple mathematics: non-numerical approaches

Numerical calculations represent the most general approach to solving differential equations in KCE, but they require a great deal of expertise in computational methods. Such expertise is not common among analytical scientists. To make KCE methods accessible to a wide scientific community, it is important to augment KCE methods with simple mathematical approaches for processing the experimental data. It should be understood that a simplified solution of a system of differential equa-

tions is only possible under certain simplifying assumptions about the interaction of L and T. The simplification of data processing, therefore, is achieved by sacrificing the generality of the approach and the accuracy of calculations.

3 Applications of KCE

3.1 Measuring binding parameters

3.1.1 Multi-method KCE toolbox

Although individual KCE methods with numerical modeling can be used for measuring binding parameters, there is always an uncertainty in the accuracy of binding parameters found from a single method – the more parameters are fitted, the higher the uncertainty. The alternative to a single KCE method is a multi-method KCE toolbox [17]. The multi-method KCE toolbox constitutes a powerful approach not only to measuring binding parameters but also to testing hypotheses about the mechanisms of biomolecular interactions. Figure 2 summarizes the general approach to the development and analytical utilization of the multi-method KCE toolbox. Conceptually, experimental electropherograms are obtained by multiple KCE methods first. A hypothetical model of interactions between L and T is suggested, and the system of differential equations (system 2) is built to describe the hypothesis. The experimental KCE electropherograms are fitted with simulated electropherograms simultaneously to obtain the best fits with one of the criteria used for non-linear regression analysis, for example, minimum chi-square. If the quality of fitting is not satisfactory, a new hypothesis is suggested for the interaction and the procedure is repeated until a satisfying hypothesis is found. The best fits for the accepted hypothesis lead to the determination of stoichiometric and kinetic parameters of the interaction.

The proof of principle for a multi-method KCE toolbox was performed with six KCE methods and a well-studied experimental system: interaction between ssDNA-binding (SSB) protein and ssDNA [17–24, 27, 33, 34, 44, 45]. First, a hypothesis was tested that SSB protein and DNA interaction is described by Eq. (1). The best fit of six experimental KCE electropherograms for this hypothesis was obtained but the deviations between experimental and simulated electropherograms were unacceptably high for three of six KCE methods (Fig. 3A), thus suggesting that hypothesis 1 was not valid. Second, another hypothesis, which was based on existing empirical data about the interaction of SSB protein and ssDNA, was tested. Two types of interactions have been previously hypothesized for SSB protein and ssDNA: high-affinity specific binding and low-affinity nonspecific binding [44, 45]. Non-specific binding was hypothesized to occur due to electrostatic attraction between SSB protein and DNA, which does not necessarily involve the DNA-binding site of SSB protein. To account for the two types of binding, reaction 1 was modified to include two types of complexes and two sets of rate constants. The system of differential equations for the formation of two types of complex was built and the experimental KCE electropherograms were then fitted with simulated ones for the new model. The best fit was found to be in satisfactory quantitative agreement with the experimental data (Fig. 3B), which allowed the acceptance of the new model and rate constants obtained from the non-linear regression analysis for the best fit. The multi-method KCE toolbox facilitated, for the first time, the determination of kinetic parameters of specific and nonspecific protein-DNA interactions.

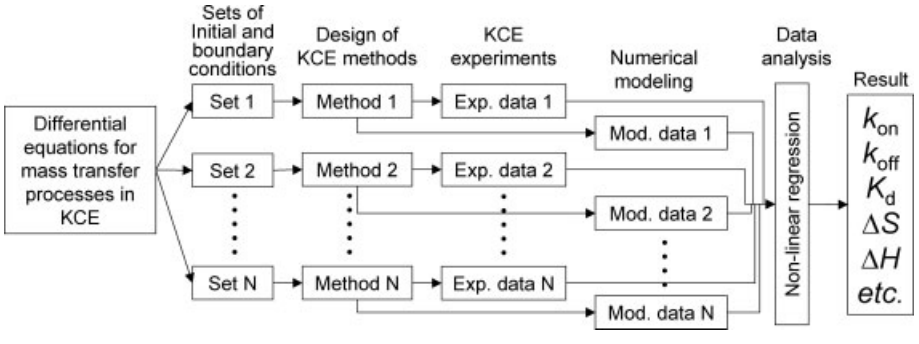

Figure 2. Flow chart depicting the general approach to the development and utilization of a multi-method KCE toolbox. First, a system of differential equations is written to describe the mass transfer processes, which are governed by intermolecular interactions and electrophoresis. Second, qualitatively independent sets of initial and boundary condition are defined to define several KCE methods. Third, KCE experiments are performed with initial and boundary conditions chosen. Fourth, simulated electropherograms are built through numerical modeling. Finally, non-linear regression is used to find kinetic and thermodynamic parameters at which simulated electropherograms fit experimental data the best.

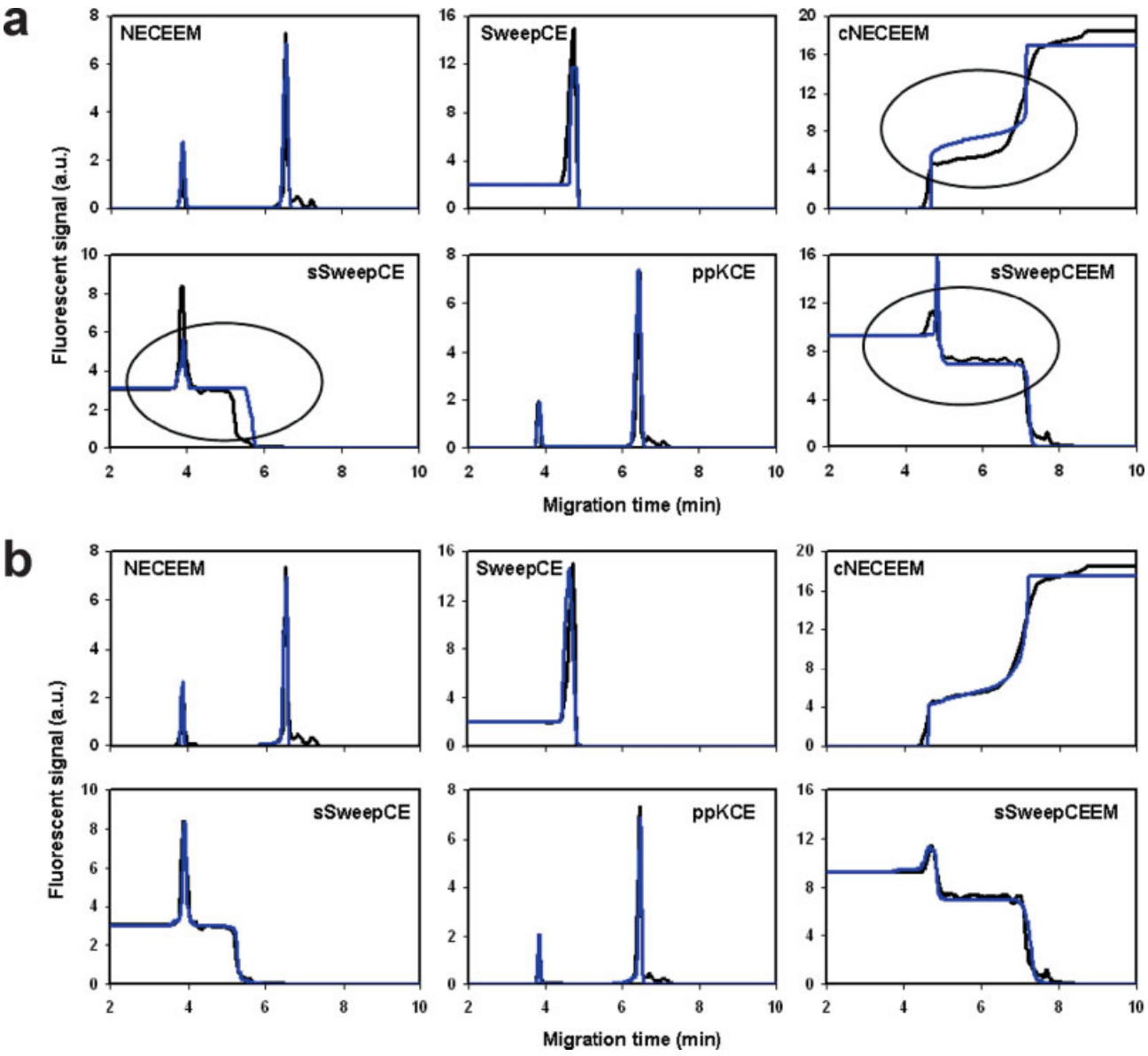

Figure 3. Application of the six-method KCE toolbox to testing hypotheses about the nature of interaction between fluorescently labeled ssDNA and SSB protein and finding rate constants of interactions. Black traces show experimental electropherograms for six KCE methods. Blue traces show simulated electropherograms corresponding to the best fitting using the minimum chi-square criterion. Experimental electropherograms are identical in both panels; simulated electropherograms differ in (a) and (b). (a) Simulated electropherograms for the unsatisfactory model, which assumes one type of interaction only; ovals indicate areas of fitting with unacceptably large deviations between experimental and simulated electropherograms. (b) Simulated electropherograms for the satisfying model, which assumes two types of interactions, specific and nonspecific.

The multi-method KCE toolbox requires simultaneously fitting experimental electrophoretic data for multiple KCE methods. This is currently performed with a custom-designed computer program. To become accessible to the majority of CE-practicing laboratories, the multi-method KCE toolbox has to be augmented with a commercial user-friendly computer program. Such a program can be potentially integrated into software packages of commercial CE instruments. We created a DLL library that allows numerical modeling of KCE using unitless variables and any initial and boundary conditions. Different interfaces can be used to work with the library; we are using Excel Spreadsheet.

3.1.2 KCE methods with simple mathematics

3.1.2.1 NECEEM

In NECEEM, an equilibrium mixture of L, T, and L·T is prepared first. Second, a short plug of the equilibrium mixture is injected by pressure into the capillary, which is free of L, T, and L·T. Third, a high voltage is applied to separate L, T, and L·T under these non-equilibrium conditions. As an example, it is assumed that the velocity of L is greater than that of T; the velocity of L·T is typically intermediate. As soon as the zones of L, T, and L·T are separated, L·T is no longer at equilibrium with L and T; it continuously dissociates with the unimolecular rate constant k_{off}. The extent of re-association of L and T decreases with increasing efficiency of their electrophoretic separation. While equilibrium fractions of L, T, and L·T migrate as short bands, L and T, which are produced from the dissociation of L·T, have exponential concentration profiles. Figure 4 depicts a schematic NECEEM electropherogram in which all peak-dispersion effects are neglected so that the peaks have ideal rectangular shapes. If re-association of L and T is negligible, system 1 can be easily solved to give algebraic equations for concentration dependencies of L, T, and L·T on the migration time to the detector [22]. Further, algebraic equations can be obtained for finding k_{off} and K_d or the concentration of T (see below) using only shapes and areas and migration times of peaks in a NECEEM electropherogram. In addition, ligands with pre-defined binding parameters can be selected from complex mixtures (*e.g.*, combinatorial libraries) if fractions are collected in specific time windows of a NECEEM electropherogram (see below).

A single NECEEM electropherogram contains data sufficient for finding K_d and k_{off}. NECEEM starts with the equilibrium mixture and, therefore, has a memory of the equilibrium, which is necessary for finding K_d. The L·T complex dissociates during NECEEM and the kinetics of complex dissociation is recorded in the smears, allowing for the calculation of k_{off}. The areas of peaks and smears in a NECEEM electropherogram are proportional to the amounts of corresponding species. A single NECEEM electropherogram can be used to find four measurable parameters required for the determination of K_d and k_{off} (Fig. 4; color-enhanced figures are available in the Supporting Information). A_1 is the area of the peak corresponding to L, which was free in the equilibrium mixture. A_2 is the area of the peak corresponding to L·T, which was still intact at the time of passing the detector. A_3 is the area of the exponential smear left by L dissociated from L·T during the separation. Finally, $t_{L\cdot T}$ is the migration time of the complex. The values of K_d and k_{off} can be calculated using the following algebraic equations or their variations [18–32]:

$$K_d = \frac{[T]_0(1 + A_1/(A_2 + A_3)) - [L]_0}{1 + (A_2 + A_3)/A_1} \quad (4)$$

and

$$k_{off} = \ln\left(\frac{A_2 + A_3}{A_2}\right)/t_{L\cdot T} \quad (5)$$

Here, $[T]_0$ and $[L]_0$ are total concentrations of T and L in the equilibrium mixture. Advantageously, areas and migration time associated with a single species only (L in this example) are required. This simplifies the use of fluorescence detection since finding a strategy for labeling a single species is relatively easy. A major step in the method development for NECEEM involves finding conditions for good-quality separation of L from L·T.

If fluorescence detection is used, the potential change of the quantum yield of fluorescence upon complex formation should be taken into consideration. Relative quantum yields of fluorescence can be measured in NECEEM in a simple procedure and included in Eqs. (4) and (5) to correct for its change through dividing the areas by the relative quantum yield [19]. When on-column detection is used, the areas must be divided by the migration times of corresponding species. These rules originate from the basic CE principles and are common for all KCE methods.

Figure 5a depicts an experimental NECEEM electropherogram for the interaction between fluorescently labeled ssDNA and SSB protein. While defining the areas, it is important to accurately define the boundary between the areas. The boundary between A_1 and A_3 can be found by comparing the peaks of free L in the presence and absence of T. Our study shows that the uncertainty in defining the boundaries between the areas leads to experimental errors in the range of 10%, which is an acceptable level of experimental errors for most applica-

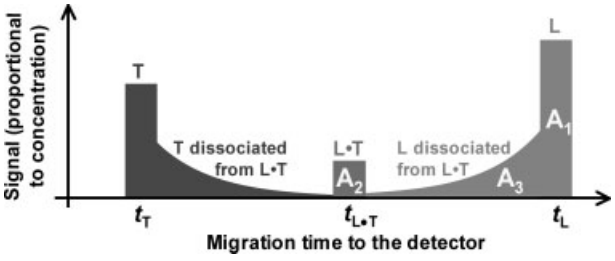

Figure 4. Schematic NECEEM or ppKCE electropherogram with experimental parameters used for quantitative measurements: A_1 is the peak area of L that either was free in the equilibrium mixture (for NECEEM) or did not form the complex during the mixing of zones of L and T (for ppKCE), A_2 is the peak area of intact L·T at the time of its passing the detector, A_3 is the peak area of L dissociated from L·T during the separation, t_L, $t_{L\cdot T}$, and t_T are migration times from the capillary inlet to the detector of L, L·T, and T, respectively.

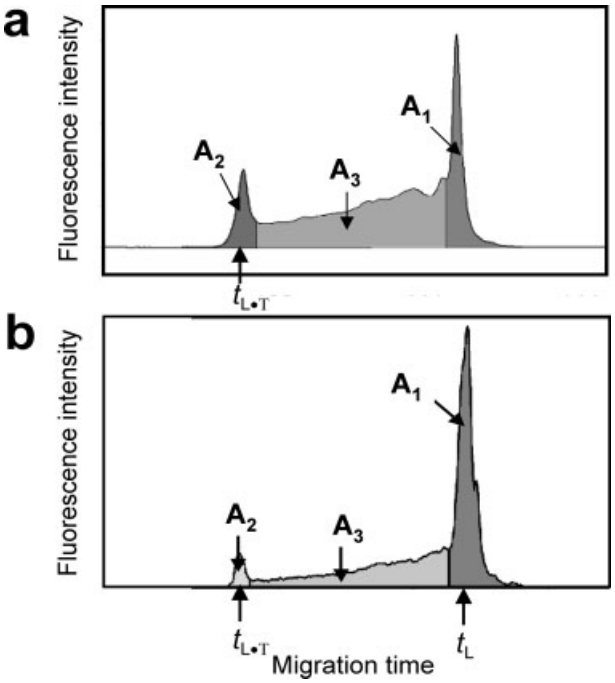

Figure 5. Example of NECEEM (a) and ppKCE (b) electropherograms for the interaction between fluorescently labeled ssDNA and SSB protein. Compare them with the schematic electropherogram in Fig. 4.

tions. Alternatively, mathematical modeling of a NECEEM electropherogram can be used to find both K_d and k_{off} from the non-linear regression analysis without the need to define the areas. We typically use the area method, as it is simple, fast, and acceptably accurate. For the same reasons, the area method is also more appealing for other researchers [46].

NECEEM-based determination of K_d and k_{off} is fast, accurate, and has a wide and adjustable dynamic range. The upper limit of K_d values depends on the highest concentration of T available and can be as high as millimolar. This allows for the measurement of K_d values for very low affinities (high K_d values), *e.g.*, bulk affinities of naïve combinatorial libraries [25, 30–32, 35]. The lower limit of K_d depends on the concentration limit of detection. For fluorescence detection, it can be as low as picomolar. The dynamic range of k_{off} values is defined by the migration time of the complex, which can be easily regulated by the length of the capillary, electric field, or electroosmotic velocity. The practically proven dynamic range of k_{off} spans from 10^{-4} to 1 s^{-1} [18, 19, 46].

Although only one electropherogram is required for finding both K_d and k_{off}, the concentration of T (if L is used as a detectable species) should be within an order of magnitude from the K_d value. Titration of T with tenfold increments in concentration is recommended as the fastest way of finding suitable T. Furthermore, conducting several experiments may be required to find the experimental deviation of the K_d value.

The equilibrium is typically established in the incubation buffer, while dissociation occurs in the electrophoresis run buffer. The values of K_d and k_{off} are, thus, measured for the incubation buffer and run buffer, respectively. If the incubation buffer and the electrophoresis run buffer are identical, then K_d and k_{off} are determined under the same conditions and k_{on} can be calculated as $k_{on} = k_{off}/K_d$. It is typically possible to match the incubation and run buffers. An example of when such matching is difficult is when T is the protein requiring the use of a high salt concentration. CE cannot tolerate high salt concentrations in the run buffer due to the high Joule heating, which can deteriorate the quality of separation.

So far, NECEEM was used to measure binding parameters for the interaction of DNA with a number of proteins (SSB protein [17–24, 27, 33, 34], MutS protein [36], tau protein [26], designed photo-controlled GCN4-bZIP protein [28], and AID protein [29]), and protein-peptide interaction [46].

3.1.2.2 ppKCE

In ppKCE, short plugs of L and T are injected into the capillary sequentially; the component with a lower mobility is injected first [17]. When the voltage is applied, the faster moving component passes through the slower moving component resulting in complex formation. Eventually, the electrophoretic zones of L and T are separated and the complex starts dissociating. The resulting electropherogram is qualitatively similar to that of NECEEM: it has peaks of L, T, and L·T and "smears" of L and T dissociated from L·T (see Fig. 4). However, since ppKCE does not start with the equilibrium mixture of L and T, the resulting electropherogram does not have a "memory" of K_d but rather has a memory of k_{on} and k_{off}. Both k_{on} and k_{off} can, thus, be calculated from a ppKCE electropherogram using areas of peaks and smears and migration times of peaks. A simple mathematical approach has been recently developed for processing the ppKCE data [34]. The approach is based on three simplifying assumptions for reaction 1. First, it is assumed that the stoichiometry of interaction between L and T is 1:1; for higher-order stoichiometries, numerical modeling of the data has to be used. Second, it is assumed that only the forward reaction occurs when the zone of T moves through that of L. Finally, there is an assumption that only the reverse process in reaction 1 occurs after the zones of L and T are separated.

Figure 4 shows a schematic ppKCE electropherogram with all measurable parameters required for k_{off} and k_{on} calculation. The complex dissociation processes are identical in NECEEM and ppKCE; therefore, approaches developed for the calculation of k_{off} in NECEEM are applicable to ppKCE as well [18, 19, 22]. For example, k_{off} can be calculated using Eq. (5), which employs only the areas and migration times. The value of k_{on} can be found from the following equation:

$$k_{on} = \varepsilon l(1/t_T - 1/t_L)/([L]l_L) \quad (6)$$

where l is the length of the capillary from the inlet to the detector; l_L is the length of the plug of L; t_L and t_T are migration times to the detector of L and T, respectively; [L] is the concentration of L in the solution it is injected from; ε is a parameter which is found from the following equation:

$$A_1/(A_1 + A_3 + A_2) = \\ = 1/\varepsilon \times \ln\{(\exp(\varepsilon) - 1)\exp(-\varepsilon \times ([T]l_T/([L]l_L))) + 1\} \quad (7)$$

where [T] is the concentration of T in solution it is injected from; l_T is the length of the plug of T; A_1 is the peak area of L that did not form the complex during the mixing of zones of L and T, A_2 is the peak area of intact L·T at the time of its passing the detector, and A_3 is the peak area of L dissociated from L·T during the separation. The easiest way to solve Eq. (6) for ε is through a numerical calculation with one of the commercially available solvers, for example a Microsoft Excel solver. The Excel spreadsheet for solving Eq. (6) can be downloaded from the Internet (www.chem.yorku.ca/profs/krylov).

The ppKCE method was used to calculate k_{on} and k_{off} for the interaction between SSB protein and fluorescently labeled ssDNA [34]. Figure 5b show an example of an experimental ppKCE electropherogram. To find the migration time of SSB protein, t_T, a separate CE experiment with SSB protein only and UV detection was conducted (not shown). The values of k_{on} and k_{off} obtained with ppKCE were in good agreement with those obtained with other methods.

In ppKCE with fluorescence detection, very low concentrations of reacting components can be used, allowing for reliable measurement of k_{on} values as high as the diffusion controlled ones ($\sim 10^9$ $M^{-1}s^{-1}$). The mixing of the reacting components in KCE methods proceeds in a pseudo-continuous mode, thus excluding "dead" time, inevitable in stopped-flow methods.

3.1.2.3 SweepCE

The concept of SweepCE is based on the sweeping of a slowly migrating component (*e.g.*, L) by a fast-migrating component (*e.g.*, T) during electrophoresis. The capillary is pre-filled with a solution of L and electrophoresis is then carried out from a solution of T in a continuous mode. Because the electrophoretic mobility of T is greater than that of L, T continuously mixes with L and forms the L·T complex (C is used instead of L·T in the mathematical equations). The complex migrates with a velocity higher than that of L and causes sweeping of L. The value of k_{on} for complex formation can be determined from the time profile of concentration of one of the interacting species (*e.g.*, L). This can be done with a simple mathematical model of the sweeping process obtained under the assumption that the dissociation process is slow enough to be neglected with respect to the process of complex formation. Under this assumption, the general solution for system 2 can be obtained analytically [33]. The resulting expression for concentrations of L, T, and C as functions of the migration time (t) and the distance from the capillary inlet (x) are shown in Eq. (8).

$$L(t,x) = L_0 \frac{\exp\left(k_{on}L_0\dfrac{x - v_L t}{v_T - v_L}\right)\theta(x - v_L t)}{\left\{\exp\left(-k_{on}T_0\dfrac{x - v_T t}{v_T - v_L}\right) - 1\right\}\theta(-x + v_T t) + \left\{\exp\left(k_{on}L_0\dfrac{x - v_L t}{v_T - v_L}\right) - 1\right\}\theta(x - v_L t) + 1}$$

$$T(t,x) = T_0 \frac{\exp\left(k_{on}T_0\dfrac{x - v_T t}{v_T - v_L}\right)\theta(x - v_T t)}{\left\{\exp\left(-k_{on}T_0\dfrac{x - v_T t}{v_T - v_L}\right) - 1\right\}\theta(-x + v_T t) + \left\{\exp\left(k_{on}L_0\dfrac{x - v_L t}{v_T - v_L}\right) - 1\right\}\theta(x - v_L t) + 1}$$

$$C(t,x) = k_{on}\int_0^t L(t - \tau, x - \tau v_c)T(t - \tau, x - \tau v_c)\mathrm{d}\tau \quad (8)$$

Here, T_0 and L_0 are the concentrations of T and L, respectively, before the start of the sweeping process; θ is the parameter which equals 0 if $x < 0$ and equals 1 if $x \geq 0$. The three expressions can be used to build simulated electropherograms. All parameters in the three expressions, except for k_{on}, are either defined (θ), or controlled (T_0, L_0), or can be found in independent CE experiments (v_T, v_L, and v_C). Therefore, fitting experimental electropherograms with the simulated ones requires the optimization of a single parameter, k_{on}, only. Standard procedures for non-linear regression of experimental data can be used for fast and accurate determination of k_{on}.

This SweepCE approach was used to find k_{on} for the interaction of fluorescently labeled ssDNA with SSB protein [33]. SweepCE electropherograms for three different concentrations of DNA are presented in Fig. 6 (blue lines). Simulated SweepCE electropherograms, which provide the best fitting of experimental data, are shown in the figure by red lines. The k_{on} value obtained from SweepCE analyses was in satisfactory agreement with k_{on} indirectly determined as $k_{on} = k_{off}/K_d$ using k_{off} and K_d obtained by NECEEM under conditions identical to the experimental conditions of the SweepCE. It is remarkable that a simple model of SweepCE can provide very good quantitative description of experimental electropherograms. The simple mathematical model of SweepCE works if complex dissociation during the time of SweepCE separation is negligible. With the shortest separation times in CE being in the order of a few seconds, the simple model can be used for finding k_{on} of complexes, whose k_{off} values are as high as 0.1 s^{-1}. For greater k_{off}, the system of partial differential equations should include the rate of complex dissociation and should be solved numerically.

Similar to ppKCE, if fluorescence detection is used in SweepCE, very low concentrations of reacting components can be used, which facilitates reliable measurement of k_{on} values as high as the diffusion controlled ones ($\sim 10^9$ $M^{-1}s^{-1}$). The mixing of the reacting components in SweepCE proceeds in a continuous mode, thus completely excluding "dead" time, inevitable for all stopped-flow methods.

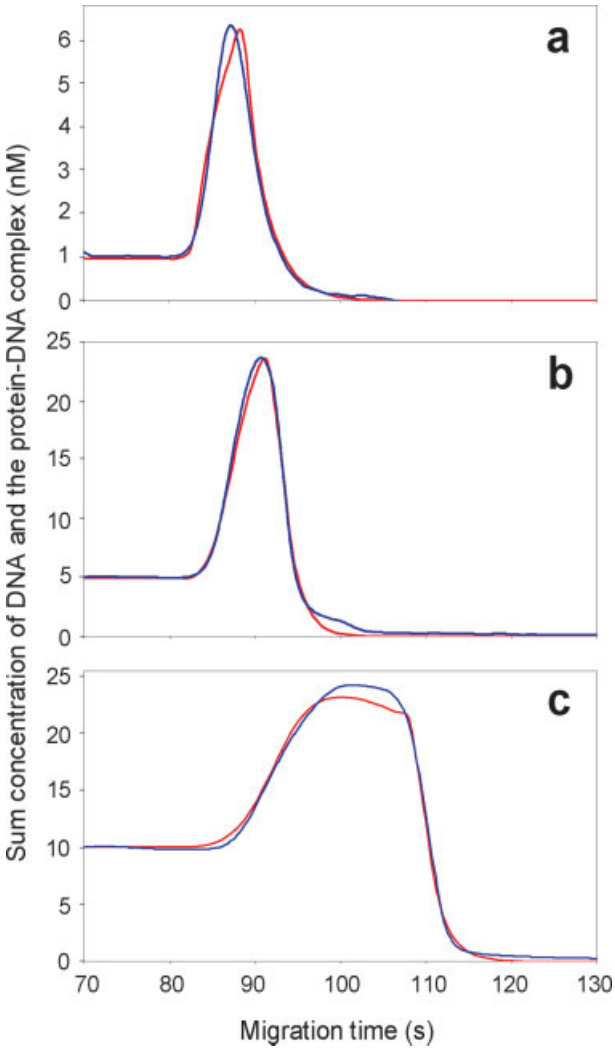

Figure 6. Example of fitting experimental SweepCE electropherograms with simulated SweepCE electropherograms. Experimental SweepCE electropherograms were obtained for the interaction between SSB protein and fluorescently labeled ssDNA at three different concentrations (increasing from a to c). Simulated SweepCE electropherograms were obtained by non-linear regression of the experimental data using the least square method. The quality of fitting is good for all three electropherograms. As the three simulations were done with the same k_{on} value this value can be considered as correct.

3.2 Temperature-controlled KCE

KCE with a well-controlled temperature inside the capillary can be used to study thermochemistry and measure ΔH and ΔS of affinity interactions. One of the problems along this way is the temperature control itself. CE is a heat-generating technique. The ability to control the temperature inside the capillary depends on the quality of heat exchange between the media inside the capillary and the environment outside the capillary. The best quality heat exchange is achieved through washing the capillary with a liquid heat exchanger. This approach has been realized in commercially available CE instruments. Depending on the amount of heat generated, heat exchange can be more or less efficient and the temperature inside the capillary can differ from that of the heat

exchanger to a certain degree. This emphasizes the need for measuring the temperature inside the capillary. Typically, spectroscopic methods are used to measure the temperature inside the capillary. They rely on the dependence of spectroscopic properties of molecular probes (such as fluorophores) on temperature. Although easy to use, spectroscopic methods have two major limitations. First, they measure temperature at the detection point only. In most of instruments, the thermostabilization of the capillary at the detection point is either less efficient than in the rest of the capillary or absent, making spectroscopic measurements inaccurate. Another limitation of spectroscopic methods is that a calibration curve needs to be built with the same instrument, which is to be calibrated; on the other hand the calibration curve can be built only with a trusted instrument. This contradiction is reminiscent of the "hen and egg" problem; to calibrate a non-trusted instrument we have to assume that it is trusted. The two limitations make spectroscopic methods of temperature determination unreliable.

3.2.1 KCE-based measurements of temperature inside the capillary

KCE offers a viable alternative to spectroscopic methods for measuring temperature inside the capillary – it is based on the dependence of one of the binding parameters, k_{on}, k_{off}, or K_d, on temperature. First, a calibration curve of "binding parameter *versus* temperature" is built for an affinity pair of choice, which can be, for example SSB protein and ssDNA, described above. Advantageously, the calibration curve does not need to be built with the CE instrument in question; it can be built with another (trusted) CE instrument or with another kind of technique, for example SPR. Then, the same binding parameter is measured in a CE instrument in question and the calibration curve is used to find the temperature. In addition to solving the "hen and egg" problem, this approach also measures an effective temperature in the total volume of the capillary, which is a more relevant value than the one measured in the detection point.

The use of KCE for measuring temperature inside the capillary has been experimentally demonstrated by measuring k_{off} as a function of temperature for the interaction between SSB protein and fluorescently labeled ssDNA [23]. The calibration curve was built with a Beckman MDQ CE instrument, which uses a liquid heat exchanger (Fig. 7). The calibration curve was then used to measure the temperature inside the capillary in a custom-built instrument with the capillary exposed to the ambient atmosphere at 20°C. It was found that the temperature inside the capillary was 35°C. As affinity interactions are very sensitive to temperature, assuming that the capillary temperature is equal to the ambient temperature could potentially lead to dramatic misinterpretations of experimental results.

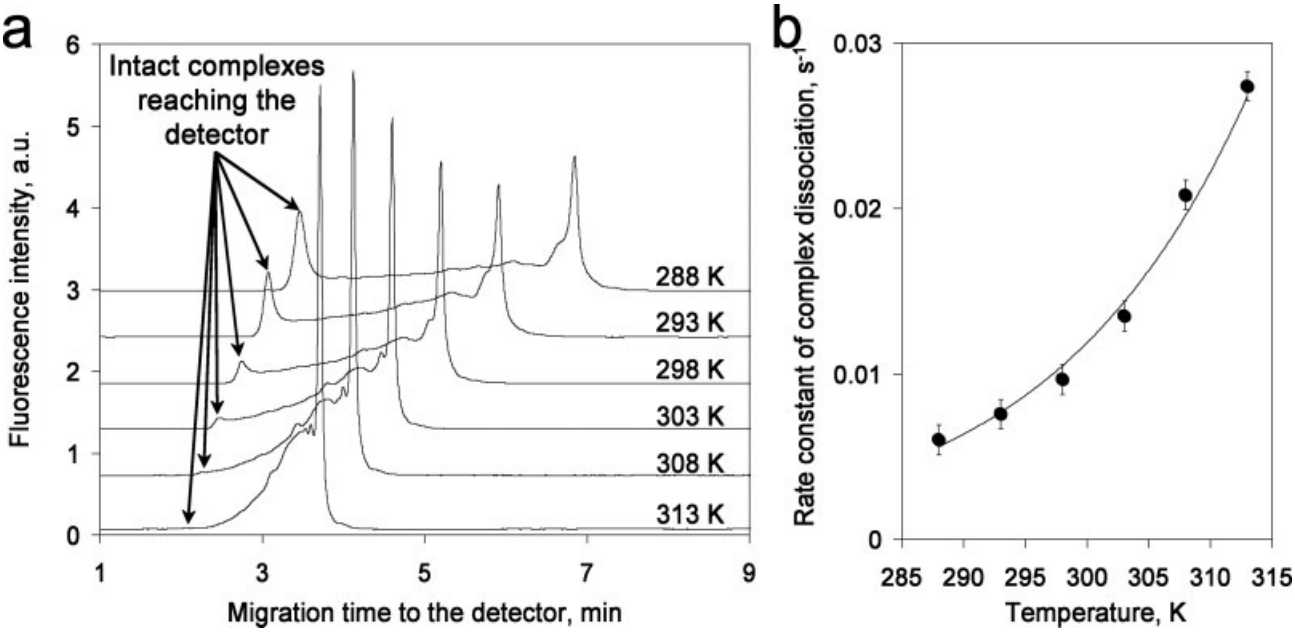

Figure 7. KCE-based determination of temperature inside the capillary. (a) Temperature dependence of NECEEM electropherograms for the interaction between SSB protein and fluorescently labeled ssDNA. The data in (a) are used to find k_{off} values for different temperatures and build a calibration curve "k_{off} *vs.* T" shown in (b).

3.2.2 Thermochemistry of interaction between *Taq* DNA polymerase and its DNA aptamer

Temperature-controlled NECEEM was used for detailed study of the thermochemistry of interaction between *Taq* DNA polymerase and its DNA aptamers. *Taq* DNA polymerase is widely used in PCR. An aptamer for the enzyme was previously selected for hot-start PCR. It binds the enzyme and inhibits it at low temperature, thus preventing the amplification of non-specific DNA hybrids. It dissociates from the enzyme, however, at higher temperatures, making the enzyme functional. Figure 8 shows temperature dependencies of three binding parameters, k_{on}, k_{off}, and K_d, and Van't Hoff plots for the calculation of ΔH and ΔS [24]. The value of K_d does not change until the temperature reaches 36°C; K_d grows rapidly with the temperature increasing above 36°C. Thus, the equilibrium stability of the complex decreases as temperature grows above 36°C. The decrease of stability can be due to two reasons: the decreased rate of complex formation, k_{on}, and the increased rate of complex dissociation, k_{off}. In this case, k_{on} changes more dramatically than k_{off}, indicating that the equilibrium stability decreases due to the decreased rate of complex formation. Most likely, the secondary structure of the aptamer starts "melting" at 36°C and loses its binding function. On the other hand, if the aptamer is bound to the protein, the protein stabilizes its structure and the temperature increase does not lead to a significant increase in the rate of complex dissociation. Thus, the knowledge of temperature dependencies of k_{on} and k_{off}, which can be obtained with KCE methods, helps us to understand mechanisms of temperature dependencies of complex stability.

3.3 Quantitative affinity analysis of the concentration of T

3.3.1 Concept of affinity measurements of concentrations

An unknown concentration of an undetectable target can be measured through its affinity reaction with a detectable ligand; the ligand in such an analysis is used as an affinity probe. Classical immunoassay and hybridization analysis are examples of such affinity measurements, with antibodies and hybridization probes as ligands [47, 48]. Typically, the kinetic and equilibrium binding parameters of interaction between L and T are unknown; instead, a calibration curve is built for the dependence of a signal (fluorescence, absorbance, radioactivity, *etc.*) from the detection of L on the concentration of T. Classical affinity methods, thus, have a general disadvantage: a new calibration curve has to be built for every new concentration of L.

KCE methods provide a calibration-free alternative to classical affinity analysis. The general theory of such measurements has not been developed yet, but their feasibility becomes clear when we notice that concentrations of T and L in the starting solution (or in the equilibrium mixture) are parameters in equations (see, for example, Eqs. 4, 6–8) used for the determination of binding parameters, k_{on}, k_{off}, and K_d. When determining the binding parameters, we assume that the concentrations of L and T are known. This problem can be reversed – if the binding parameters are known, the unknown concentration of T can be found. The problem can be considerably simplified if the concentration of the affinity probe L is also known, which is typically easy to measure. KCE methods with a developed apparatus for

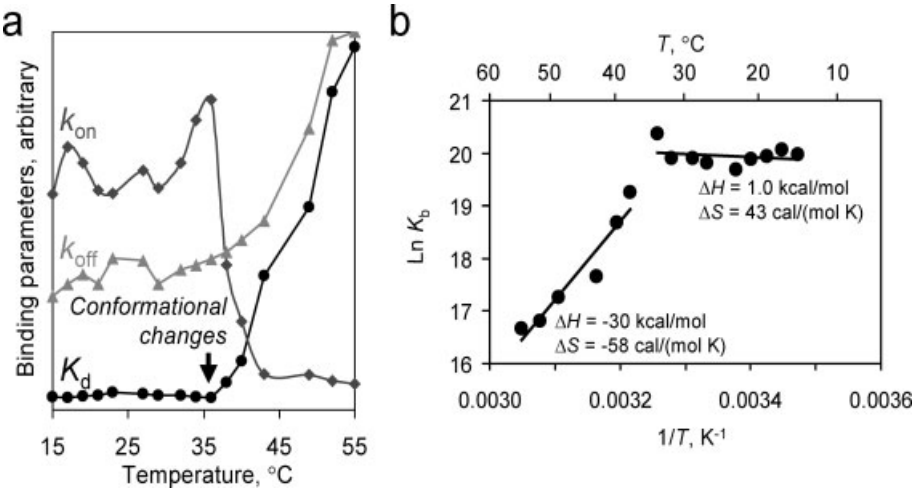

Figure 8. KCE-based study of thermochemistry of interaction between *Taq* DNA polymerase and its DNA aptamer. (a) Temperature dependencies of k_{on}, k_{off}, and K_d. The data suggest that the decrease of affinity (increase of K_d) at temperature above 36°C is mainly due to less efficient binding (decreasing k_{on}) rather than more efficient dissociation (increasing k_{off}). (b) Van't Hoff plot obtained from data in (a) and used for the determination of ΔS and ΔH for this interaction.

simple mathematics are immediately applicable to calibration-free affinity measurements of the unknown concentration of T.

This review describes affinity measurements of concentrations by two methods only: NECEEM and SweepCE. It is important to emphasize that every KCE method can be used for quantitative measurements of concentrations if the kinetic nature of the method is appreciated and the experimental results are analyzed accordingly. Comparative analysis of different KCE methods would considerably enrich our understanding of KCE capabilities in this important application. An effort is now needed in developing the general theory of KCE-based affinity analyses of concentrations.

3.3.2 NECEEM

NECEEM appears to be the simplest KCE method for affinity-based measurements of the concentration of T. If the K_d value is known, the unknown concentration of T can be found from an algebraic equation obtained by rearranging Eq. (4):

$$[T]_0 = K_d \frac{A_2 + A_3}{A_1} + [L]_0 \frac{1}{1 + A_1/(A_2 + A_3)} \quad (9)$$

Advantageously, NECEEM does not require a typical calibration procedure; the K_d value serves as a "calibration" parameter. This equation includes the concentration of L and requires no re-calibration if the concentration of L changes, which is often required to change the dynamic range of the method. Furthermore, the method can be used even if the L·T complex completely dissociates during separation (Fig. 9). In this case, $A_2 \approx 0$ and Eq. (4) reduces to [20]:

$$[T]_0 = K_d \frac{A_3}{A_1} + [L]_0 \frac{1}{1 + A_1/A_3} \quad (10)$$

Due to this feature, ligands with high k_{off} values can still be used for quantitative affinity analyses by NECEEM. This also makes the method applicable to systems in which L·T migrates so slowly, that L·T dissociates to an undetectable level by the time it reaches the detector (see Fig. 9).

When the k_{off} value is much lower than the reciprocal migration time of L·T, no detectable dissociation of L·T occurs and only the peaks of L and L·T are observed (no smears are detected). An example of this is a NECEEM-based hybridization analysis, in which DNA or RNA of interest is detected with a fluorescently labeled DNA hybridization probe (Fig. 10) [21, 38]. In this case, the dissociation constant can be as low as 10^{-30}–10^{-40} M and

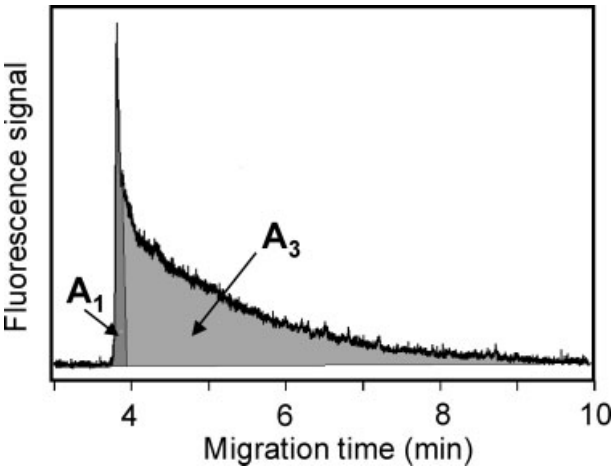

Figure 9. Example of NECEEM-based measurement of T using L as an affinity probe (T is thrombin and L is its aptamer). Under the experimental conditions used T migrates slower than L and no peak of L·T is detected as most of L·T dissociates before it reaches the detector and cannot be detected ($A_2 = 0$).

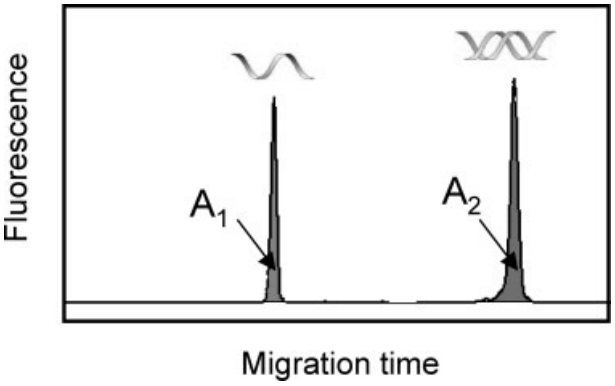

Figure 10. Example of NECEEM-based measurement of T using L as an affinity probe for the DNA hybridization reaction: T is DNA and L is a fluorescently labeled DNA probe. Dissociation of the DNA hybrid is very slow so that it is not detectable ($A_3 = 0$).

k_{off} is negligibly small. Thus, both K_d and A_3 can be assumed to equal zero, and Eq. (4) can be reduced to a stoichiometry-controlled one:

$$[T]_0 = [L]_0 \frac{A_2}{A_1 + A_2} \quad (11)$$

NECEEM-based quantitative affinity and hybridization analyses are simple, fast, and accurate. The limit of detection is defined by the sensitivity of the detection system used. For best systems utilizing laser-induced fluorescence detection, the mass limit of detection can be as low as one thousand molecules, while the concentration limit of detection can reach picomoles per liter.

Another advantage of the NECEEM-based affinity and hybridization analyses is that they do not require calibration. If the K_d value is in the range of the measured target concentration, knowledge of K_d is required as Eq. (4) or (5) is used. If K_d is much less than the measured target concentration, no calibration and no knowledge of K_d are required [38].

DNA aptamers as affinity probes considerably enrich the capabilities of KCE in analyses of a variety of targets. Aptamers have a number of advantages over antibodies. First, DNA aptamers are highly negatively charged and, thus, they do not adhere to the bare silica of uncoated capillaries. Second, aptamers are relatively small molecules; this simplifies the separation of free DNA (L) from the DNA-target complex (L·T). Third, aptamers can be chemically synthesized; moreover, this synthesis is now commercially available at a very low cost. Fourth, aptamers can be easily end-labeled with fluorophores without affecting the aptamer-target interaction, which facilitates their fluorescence detection. If constant regions (used for PCR amplification) are not truncated, quantitative PCR can be used to quantitatively detect aptamers, thus, improving the limit of detection to as few as a hundred molecules [49]. Advantageously, aptamers can be selected using KCE methods (see below).

3.4 Kinetic selection of ligands

3.4.1 Concept of smart ligands

Selection of target-binding ligands from combinatorial libraries (and other complex mixtures) is one of the mainstream approaches in identifying leads for drugs and affinity probes. Typically, affinity chromatography or filtration is used for the partitioning of binders from non-binders [4, 50]. Affinity chromatography suffers from a relatively high background level; the background is defined as the relative amount of non-binders collected in the absence of the target. Moreover, conventional partitioning methods can hardly be used for selection of "smart" ligands, *i.e.*, ligands with pre-defined values of k_{on}, k_{off}, and K_d. Smart ligands will be required for the development of drugs with pre-defined pharmacokinetics and for designing detection schemes with controlled and wide dynamic ranges. Therapeutic agents, which act over different periods of time, are one of the possible applications of such smart ligands. Ligands with fast k_{on} and fast k_{off} could be used as pharmaceutical agents for acute disorders, while ligands with slow k_{on} and slow k_{off} are preferable for treating chronic diseases. An accurate quantitation of a target in the range of concentrations from 1 pM to 1 mM requires a panel of affinity probes with a similar (9 orders of magnitude) range of affinities (K_d). Diverse analytical and biomedical applications may also require ligands with different rate constants of complex dissociation (k_{off}). Initially, the idea of exploiting a set of ligands with different affinities for the same target (protein) was raised in proteomic research and the development of protein microarrays [51]. As concentrations of proteins in real samples vary significantly, affinity probes need to be modified so that lower-affinity ligands are used for highly expressed proteins and higher affinity ligands are used for proteins with low expression levels. Antibodies proved to be an unreliable ligand in such detection schemes as there are no simple ways of modifying the affinity of antibodies. The inability to develop panels of smart antibodies emphasizes the need to look at other types of ligands, preferably those that can be chemically synthesized. DNA aptamers are examples of such ligands with multiple advantages over antibodies (see above). Most of work on selecting smart ligands focused so far on the selection of smart aptamers [25, 30, 35].

3.4.2 Selection of smart ligands by NECEEM

Smart ligands are selected from highly diverse combinatorial libraries; it is assumed that ligands with desirable binding parameters are present in the library. First, it is necessary to find a CE run buffer that separates T from the combinatorial library but does not separate the components of the library. In other words, the library has to migrate as a single electrophoretic zone in such a buffer. The diversity of the chemical structures of species within the library typically makes the peak of the library relatively wide. The goal is to find separation conditions under which the peak of T is very well separated from the wide peak of the library. T is then mixed with the combinatorial library of L and incubated to obtain the equilibrium mixture. A plug of the equilibrium mixture is injected into the capillary and high voltage is applied to separate free L from the L·T complexes. To ensure a reasonable amount of the collected ligands, the diameter of the capillary is typically chosen to be greater than that in kinetic measurements and quantitative affinity analyses. Finally, fractions are collected in different time windows within the range between peaks of L and L·T. The closer the time window is to the peak of L, the more weak ligands (with high k_{off}) there are in the fraction. The closer the collection window is to the peak of L·T, the more strong aptamers (with low k_{off}) there are in the fraction. Figure 11 schematically illustrates the selection of smart ligands with pre-defined k_{off} by NECEEM. The selection of smart ligands requires multiple rounds of selection for tuning the range of parameters approximately within the following inequality:

$$\frac{1}{t_{L\cdot T}}\frac{t_T - t_{L\cdot T}}{t_L - t_1} > k_{off} > \frac{1}{t_{L\cdot T}}\frac{t_L - t_{L\cdot T}}{t_L - t_2} \quad (12)$$

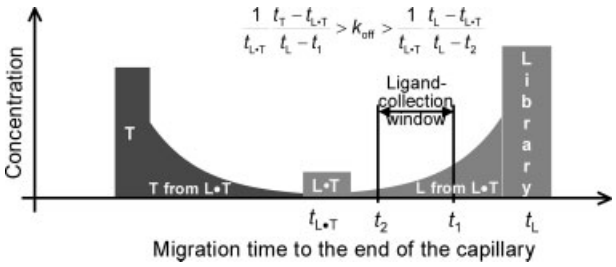

Figure 11. Schematic representation of selection of smart ligands with pre-defined k_{off} by NECEEM. The schematic NECEEM electropherogram is identical to electropherograms on Fig. 4; see legend to Fig. 4 for details. The width and position of the ligand-collection window define the range of k_{off} values of ligands in the collected fraction.

Strictly speaking, if the library contained an infinite number of ligands with a continuum of k_{off} values and if an infinite number of selection rounds were performed, ligands would be selected with a narrowing range of k_{off} around the following value:

$$k_{off}^{\infty} = \frac{t_L - t_{L\cdot T}}{t_{L\cdot T}(t_2 - t_1)} \ln\left(\frac{t_L - t_1}{t_L - t_2}\right) \quad (13)$$

In contrast to a schematic electropherogram depicted in Fig. 11, real NECEEM electropherograms contain non-rectangular peaks with more or less significant fronting and tailing. As a result, the background of the selection procedure is a strong function of the position of the fraction collection window. Figure 12 illustrates this statement; it contains a modeled NECEEM electropherogram with gaussian peaks of the library and L·T [25]. For the wider fraction collection window, non-binders from the library "leak" into the window and result in a background of 10^{-3}. A small shift of the right boundary of the fraction collection window to the left decreases the background by two orders of magnitude, while the efficiency of the collection of binders decreases only slightly (from 0.7 to 0.6).

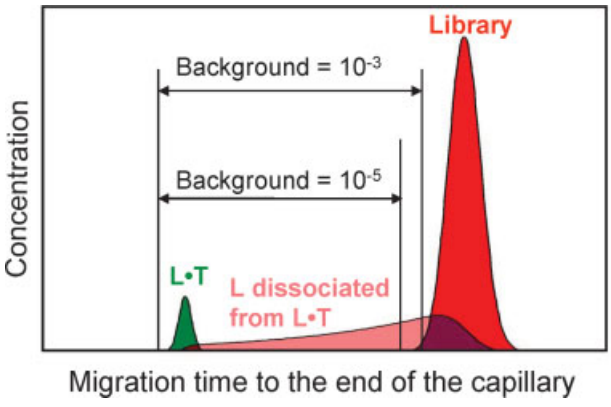

Figure 12. Schematic representation of the influence of the fraction-collection window on the background of the ligand-selection procedure in NECEEM. The shape of the peaks in this simulated NECEEM electropherogram is gaussian. The background corresponds to free L that "leaks" into the fraction-collection window even without T.

The principle of NECEEM-based selection of smart ligands was proved with the selecting of smart DNA aptamers [30]. Aptamers are DNA or RNA oligonucleotides, which can strongly bind targets with high selectivity. They have the potential to replace antibodies in all their analytical and therapeutic applications. Aptamers are selected from libraries of random DNA (RNA) sequences in multiple rounds of alternating partitioning and PCR amplification. Typically, more than ten rounds are required for aptamer selection. It was recently demonstrated that NECEEM can facilitate selection of aptamers (non-smart) in a single round of selection [25].

Smart aptamers with pre-defined ranges of k_{off} values were selected for MutS protein as a target. Fractions were collected in two rounds of selection within two ligand-collection windows (Fig. 13). Every round of selection

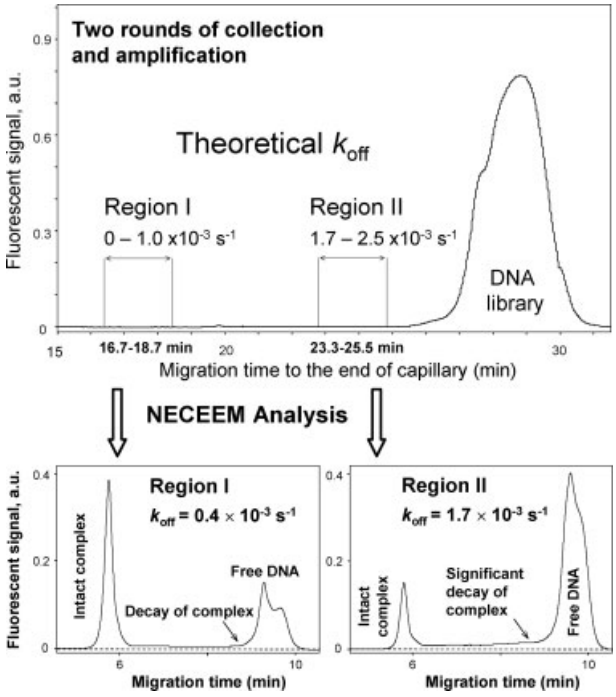

Figure 13. NECEEM-based selection of two pools of smart aptamers with different and pre-determined k_{off} values. The upper panel shows two fraction-collection region with respect to the peak of the DNA library with the corresponding theoretical k_{off} values. The two lower panes show NECEEM-based binding analyses of enriched pools of aptamers collected within the two regions along with the bulk k_{off} values.

consisted of NECEEM separation, fraction collection, PCR amplification, separation of strands, and measuring the bulk affinity of the enriched library with NECEEM. In region I, the theoretically predicted range of k_{off} was 0–1.0×10^{-3} s^{-1}, and in region II it was 1.7×10^{-3}–2.5×10^{-3} s^{-1}. After two rounds of selection in regions I and II, the pools of DNA had the experimental bulk k_{off} values of 0.4×10^{-3} and 1.7×10^{-3} s^{-1}, respectively. Thus, the theoretical consideration was proven experimentally.

3.4.3 Selection of smart ligands by ECEEM

While NECEEM can be used to select smart ligands with pre-defined k_{off} values, ECEEM facilitates selection of smart ligands with pre-defined K_d values [35]. Conceptually, the capillary is filled with a solution of the target and a plug of the equilibrium mixture of the target and the library is injected into the capillary. The high voltage is applied and the target-ligand complexes migrate under the conditions of quasi-equilibrium, meaning that ligands spend some time within the complex and some time as free molecules. If it is assumed that k_{off} and k_{on} are high enough to maintain the quasi-equilibrium between complexes and free molecules, the effective migration time t of the ligand will depend on K_d and the concentration of free target $[T]_{free}$ in the following way:

$$\frac{1}{t} = \frac{1}{t_L}\frac{K_d}{[T]_{free} + K_d} + \frac{1}{t_{L\cdot T}}\frac{[T]_{free}}{[T]_{free} + K_d} \quad (14)$$

The effective migration time of the ligand can change between $t_{L\cdot T}$ and t_L depending on K_d and $[T]_{free}$. $[T]_{free}$ is assumed to be equal to the overall concentration of the target [T] because of the constant supply of the target from the run buffer. As a result, the interaction of the library with a constant flow of the target distributes ligand molecules along the capillary according to their K_d values:

$$K_d(t) = [T]\frac{t_L}{t_{L\cdot T}}\frac{t - t_{L\cdot T}}{t_L - t} \quad (15)$$

Ideally, ligands with the same K_d values should migrate as a single peak with a small width (Fig. 14). Thus, Eq. (2) allows one to calculate a theoretical range of K_d values in a fraction collected between times t_1 and t_2:

$$[T]\frac{t_L}{t_{L\cdot T}}\frac{t_2 - t_{L\cdot T}}{t_L - t_1} > K_d > [T]\frac{t_L}{t_{L\cdot T}}\frac{t_1 - t_{L\cdot T}}{t_L - t_1} \quad (16)$$

Experimentally, peak broadening and nonspecific interactions with other components in the system may introduce a bias of unbound ligands into the collected fraction. That is why the selection procedure may require a few rounds of selection to approach the theoretically predicted K_d values. However, well-optimized CE separation conditions, such as the choice of the running buffer and capillary coatings, will ensure the minimal effect of diffusion and nonspecific interactions upon the predicted distribution of species along the capillary during the run.

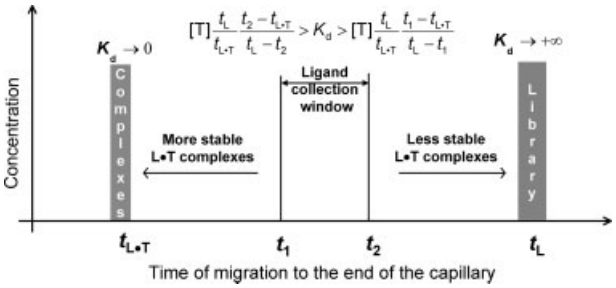

Figure 14. Concept of selection of smart ligands with pre-defined K_d by ECEEM. The maximum fraction-collection window spans from the migration time $t_{L\cdot T}$ of complexes with $K_d \to 0$ to the migration time t_L of the free library. Ligands collected in the time window t_1–t_2 in an iterative fashion will have K_d values defined by the equation in the figure.

The unique feature of ECEEM for the selection of ligands arises from its simple mathematical description. The range of the affinity distribution along the capillary is determined by [T], $t_{L\cdot T}$, and t_L. By changing these parameters, it is theoretically possible to select from the combinatorial libraries ligands with affinities ranging from picomolar to millimolar values of K_d, which covers nine orders of magnitude. It should be noted that the simple mathematical description only works under the assumption of quasi-equilibrium: the re-equilibration time in reaction 1 should be much shorter than the characteristic time of electrophoretic separation.

The experimental evaluation of ECEEM was done for selection of DNA aptamers for MutS protein [35]. Fractions were collected within three ligand-collection windows (Fig. 15) in three rounds of selection. Each round consisted of ECEEM separation, fraction collection, PCR amplification, separation of strands, and measuring the bulk affinity of the enriched library with NECEEM. After the last round of selection, the three pools of aptamers were cloned into bacteria. Selected bacterial clones were screened for the aptamer insert into the plasmids, and individual aptamers were obtained. As the next step, K_d and k_{off} values of individual sequences were measured with NECEEM. Figure 16 shows NECEEM electropherograms and binding parameters for six aptamers: three with similar K_d values and varying k_{off} and three with similar k_{off} values and varying K_d. Changing K_d affected the ratios between free DNA and the complex (Figs. 16a–c), while changing k_{off} influenced the ratio between the intact and dissociated complex (Figs. 16d–f).

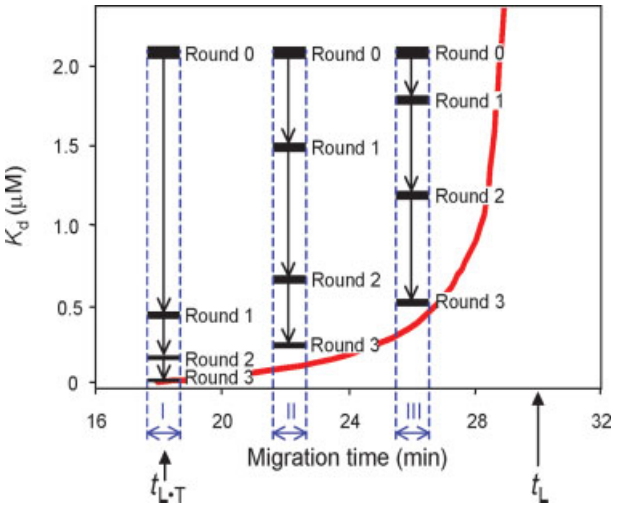

Figure 15. Affinity convergence to the theoretically predicted (red line) in three rounds of ECEEM-based selection of aptamers (black). Fractions were collected in three ligand-collection windows (blue). Round refers to one round of SELEX that involves one step of partitioning and one step of PCR amplification.

KCE-based methods of aptamer selection are characterized by exceptionally high efficiency of partitioning of aptamers from non-aptamers. For the overall aptamer-selection procedure to be efficient, the high efficiency of new partitioning methods has to be matched by high efficiency of PCR. PCR amplification of random DNA libraries used in aptamer selection has been recently studied in detail [40]. With CE as an analytical tool, fundamental differences between PCR amplification of homogeneous DNA templates and that of large libraries of random DNA sequences were found. Product formation for a homogeneous DNA template proceeds until primers are exhausted. With a random DNA library as a template, product accumulation stops when PCR primers are still in excess of the products. The products then rapidly convert to by-products and virtually disappear after only five additional cycles of PCR. The yield of the products decreases with the increasing length of DNA molecules in the library. It was also proven that the initial number of DNA molecules in PCR mixture has no effect on the by-products formation. The increase of the *Taq* DNA polymerase concentration in the PCR mixture selectively increases the

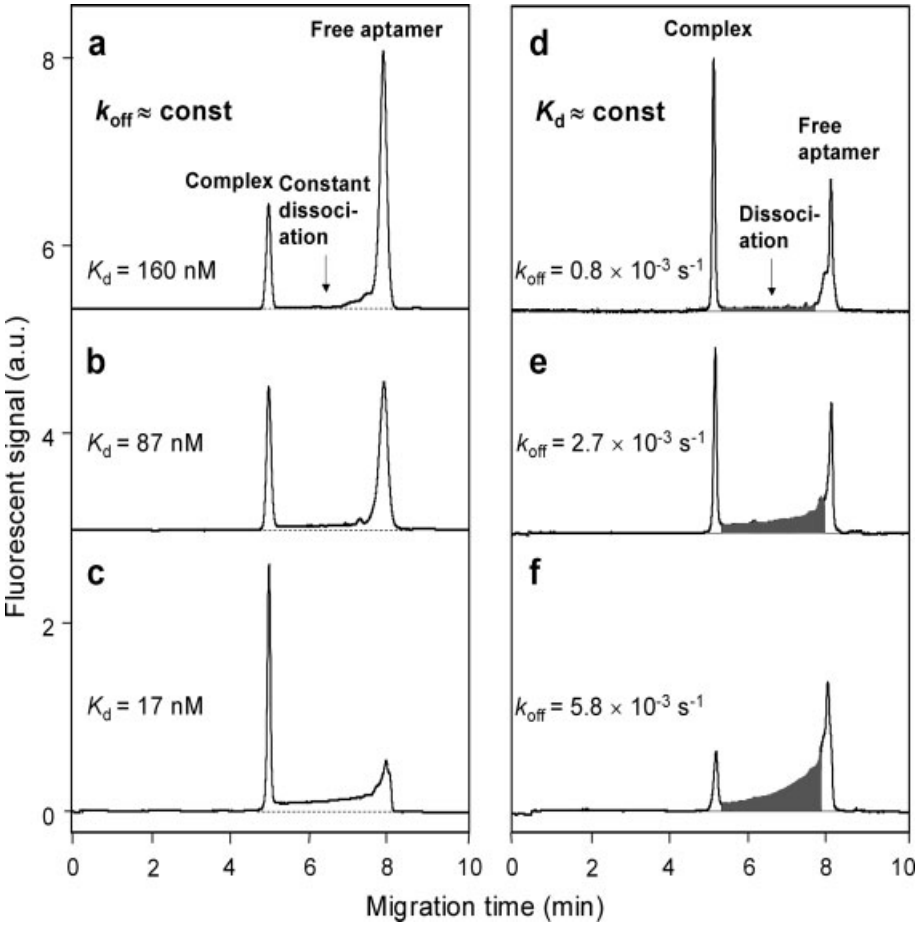

Figure 16. NECEEM electropherograms illustrating binding of six different aptamers to MutS protein. (a–c) Aptamers with similar k_{off} values, but varying K_d values. (d–f) Aptamers with similar K_d values, but different k_{off} values.

yield of PCR products. These findings suggest that standard procedures of PCR amplification of homogeneous DNA samples cannot be transferred to PCR amplification of random DNA libraries; to ensure highly efficient selection, PCR has to be optimized for the amplification of random DNA libraries.

3.4.4 Prospective of KCE methods in selection of smart ligands

Selection of smart ligands by KCE methods can be considered to still be in its infancy – only NECEEM and ECEEM have been evaluated and only in application to selection of DNA aptamers. Due to the importance of oligonucleotide aptamers, the work on the selection of aptamers will certainly continue and other KCE method will be adopted for this application. A Non-SELEX (SELEX stands for systematic evolution of ligands by exponential enrichment) process was recently invented for the selection of aptamers [31, 32]. In contrast to SELEX, Non-SELEX does not involve intermediate steps of amplification of aptamers (typically by PCR) between the rounds of partitioning of aptamers from non-aptamers. Non-SELEX is faster than SELEX but the number of steps in Non-SELEX is currently limited to three or four due to a partial sampling of collected aptamers. Due to this restriction, Non-SELEX has limited capabilities with respect to selection of smart aptamers as the latter may require more than three or four partitioning steps to tune the binding parameters to narrow ranges. Future efforts will aim at overcoming this limitation of Non-SELEX to make it fully applicable to selection of smart aptamers.

If Non-SELEX proves to be able to select smart DNA aptamers, the technology will be eventually adopted to the selection of smart ligands from non-DNA libraries. The challenges lie in the ability to (i) separate a library from the target without separating the components of the library between themselves, and (ii) arrange for sensitive detection when fluorescence detection cannot be used (it is impossible to fluorescently label small molecules without affecting their binding ability to the target). NECEEM and ECEEM can be immediately applied to the selection of ligands from libraries of small molecules tagged with DNA (DNA sequence barcodes the structure of the small molecule is attached to) [52, 53]. The electrophoretic properties of such libraries are defined largely by the DNA tag rather than the small molecule; thus, they are similar to those of pure DNA libraries. KCE methods promise a great potential in the development of smart drug candidates and smart affinity ligands of different natures.

4 Conclusions

KCE establishes a new paradigm: “Separation methods can be used as comprehensive kinetic tools”. Most previous attempts to use chromatography and electrophoresis for studying biomolecular interactions were restricted to assuming equilibrium between interacting molecules [11, 12]. Such an assumption dramatically limits applications for measuring equilibrium constants only. Furthermore, this assumption is theoretically wrong since separation disturbs equilibrium. KCE is based on the paradigm that kinetics must be appreciated when separation methods are used for studies of biomolecular interactions. As demonstrated with KCE, appreciation of kinetics significantly enriches the analytical capabilities of the methods.

Future KCE work will focus on: (i) detailed study of recently introduced KCE methods, (ii) development of new KCE methods, (iii) development of KCE tools for studying binding stoichiometry, (iv) development of simple mathematics for KCE methods, (v) application of KCE methods to new target-ligand systems, and (vi) application of KCE methods to the development of drugs and affinity probes. An important step will be the extension of KCE methods to other ways of detection, in particular, to MS. The challenge here is the limit of detection of MS, which is still several orders of magnitude below than that of fluorescence detection. An important task will be designing a system of descriptive names for KCE methods. A joint work of teams, which use electrophoresis for affinity studies, will be needed. Clarity of the nomenclature is required for KCE methods to become attractive to a wide community of molecular scientists.

Methods of KCE use a single instrumental platform and a single conceptual platform for solving multiple tasks of affinity methods. Due to their comprehensive analytical capabilities, KCE methods have the potential to become a workhorse in many areas of affinity measurements and affinity purification. This makes KCE methods highly attractive for the pharmaceutical industry as a novel approach to selection and characterization of drug candidates and affinity probes.

5 References

[1] Pearson, W. H., Berry, D. A., Stoy, P., Jung, K.-Y., Sercel, A. D., *J. Org. Chem.* 2005, *70*, 7114–7122.

[2] Okerberg, E. S., Wu, J., Zhang, B., Samii, B. *et al.*, *Proc. Natl. Acad. Sci. USA* 2005, *102*, 4996–5001.

[3] Licitra, E. J., Liu, J. O., *Proc. Natl. Acad. Sci. USA* 1996, *93*, 12817–12821.

[4] Tuerk, C., Gold, L., *Science* 1990, *249*, 505–510.

[5] Yuan, J., Wang, G., *Trends Anal. Chem.* 2006, *25*, 490–500.

[6] Kawatake, S., Nishimura, Y., Sakaguchi, S., Iwaki, T., Dohura, K., *Biol. Pharmaceut. Bull.* 2006, *29*, 927–932.

[7] Hesselberth, J. R., Miller, D., Robertus, J., Ellington, A. D., *J. Biol. Chem.* 2000, *275*, 4937–4942.

[8] Hanora, A., Bernaudat, F., Plieva, F. M., Dainiak, M. B. *et al.*, *J. Chromatogr. A* 2005, *1087*, 38–44.

[9] Tian, Y., Chen, Y., Song, D., Liu, X. *et al.*, *Anal. Chim. Acta* 2005, *551*, 98–104.

[10] Cooper, M. A., *J. Mol. Recognit.* 2004, *17*, 286–315.

[11] Heegaard, N. H. H., Nissen, M. H., Chen, D. D. Y., *Electrophoresis* 2002, *23*, 815–822.

[12] Chu, Y. H., Avila, L. Z., Biebuyck, H. A., Whitesides, G. M., *J. Med. Chem.* 1992, *35*, 2915–2917.

[13] Mitchell, P., *Nat. Biotechnol.* 2002, *20*, 225–229.

[14] Wilson, W. D., *Science* 2002, *295*, 2103–2105.

[15] Homola, J., Vaisocherowa, H., Dostalek, J., Piliarik, M., *Methods*, 2005, *37*, 26–36.

[16] Boozer, C., Kim, G., Cong, S., Guan, H., Londergan, T., *Curr. Opin. Biotechnol.* 2006, *17*, 400–405.

[17] Petrov, A., Okhonin, V., Berezovski, M., Krylov, S. N., *J. Am. Chem. Soc.* 2005, *127*, 17104–17110.

[18] Berezovski, M., Krylov, S. N., *J. Am. Chem. Soc.* 2002, *124*, 13674–13675.

[19] Krylov, S. N., Berezovski, M., *Analyst* 2003, *128*, 571–575.

[20] Berezovski, M., Nutiu, R., Li, Y., Krylov, S. N., *Anal. Chem.* 2003, *75*, 1382–1386.

[21] Berezovski, M., Krylov, S. N., *J. Am. Chem. Soc.* 2003, *125*, 13451–13454.

[22] Okhonin, V., Krylova, S. M., Krylov, S. N., *Anal. Chem.* 2004, *76*, 1507–1512.

[23] Berezovski, M., Krylov, S. N., *Anal. Chem.* 2004, *76*, 7114–7117.

[24] Berezovski, M., Krylov, S. N., *Anal. Chem.* 2005, *77*, 1526–1523.

[25] Berezovski, M., Drabovich, A., Krylova, S. M., Musheev, M. *et al.*, *J. Am. Chem. Soc.* 2005, *127*, 3165–3171.

[26] Krylova, S. M., Musheev, M., Nutiu, R., Li, Y. *et al.*, *FEBS Lett.* 2005, *579*, 1371–1375.

[27] Pang, Z., Liu, X., Al-Mahrouki, A., Berezovski, M., Krylov, S. N., *Electrophoresis* 2006, *27*, 1489–1494.

[28] Woolley, G. A., Jaikaran, A., Berezovski, M., Calarco, J. D. *et al.*, *Biochemistry* 2006, *45*, 6075–6084.

[29] Larijani, M., Petrov, A. P., Krylov, S. N., Martin, A., *J. Biol. Chem.* 2006, in press.

[30] Drabovich, A., Berezovski, M., Krylov, S. N., *Anal. Chem.* 2006, *78*, 3171–3178.

[31] Berezovski, M. V., Musheev, M. U., Drabovich, A. P., Jitkova, J. V., Krylov, S. N., *Nat. Protocols* 2006, *1*, 1359–1369.

[32] Berezovski, M., Musheev, M., Drabovich, A., Krylov, S. N., *J. Am. Chem. Soc.*, 2006, *128*, 1410–1411.

[33] Okhonin, V., Berezovski, M., Krylov, S. N., *J. Am. Chem. Soc.* 2004, *126*, 7166–7167.

[34] Okhonin, V., Petrov, A., Berezovski, M., Krylov, S. N., *Anal. Chem.* 2006, *78*, 4803–4810.

[35] Drabovich, A., Berezovski, M., Krylov, S. N., *J. Am. Chem. Soc.* 2005, *127*, 11224–11225.

[36] Drabovich, A., Krylov, S. N., *Anal. Chem.* 2006, *78*, 2035–2038.

[37] Drabovich, A., Krylov, S. N., *J. Chromatogr. A* 2004, *1051*, 171–175.

[38] Al-Mahrouki, A. A., Krylov, S. N., *Anal. Chem.* 2005, *77*, 8027–8030.

[39] Okhonin, V., Liu, X., Krylov, S. N., *Anal. Chem.* 2005, *77*, 5925–5929.

[40] Musheev, M. U., Krylov, S. N., *Anal. Chim. Acta* 2006, *564*, 91–96.

[41] Avila, L. Z., Chu, Y. H., Blossey, E. C., Whitesides, G. M., *J. Med. Chem.* 1993, *36*, 126–133.

[42] Ermakov, S., Mazhorova, O., Popov, Y., *Informatica* 1992, *3*, 173–197..

[43] Fang, N., Chen, D. D. Y., *Anal. Chem.* 2005, *77*, 849–847.

[44] Hagmar, P., Dahlman, K., Takahashi, Mi., Carlstedt-Duke, J. *et al.*, *FEBS Lett.* 1989, *253*, 28–52.

[45] Ferrari, M. E., Bujalowski, W., Lohman, T. M., *J. Mol. Biol.* 1994, *236*, 106–123.

[46] Yang, P., Whelan, R. J., Jameson, E. E., Kurzer, J. H. *et al.*, *Anal. Chem.* 2005, *77*, 2482–2489.

[47] Ohmura, N., Tsukidate, Y., Shinozaki, H., Lackie, S. J., Saiki, H., *Anal. Chem.* 2003, *75*, 104–110.

[48] Ferguson, J. A., Boles, T. C., Adams, C. P., Walt, D. R., *Nat. Biotechnol.* 1996, *14*, 1681–1684.

[49] Zhang, H., Wang, Z., Li, X.-F., Le, X. C., *Angew. Chem. Int. Ed. Engl.* 2006, *45*, 1576–1580.

[50] Hodgson, R. J., Chen, Y., Zhang, Z., Tleugabulova, D. *et al.*, *Anal. Chem.* 2004, *76*, 2780–2790.

[51] Barry, R., Soloviev, M., *Proteomics* 2004, *4*, 3717–3726.

[52] Kanna, M. W., Rozenman, M. M., Sakurai, K., Snyder, T. M., Liu, D. R., *Nature* 2004, *431*, 545–549.

[53] Garner, Z. J., Tse, B. N., Grubina, R., Doyon, J. B. *et al.*, *Science* 2004, *305*, 1601–1605.

